33RD CONGRESS
OF THE INTERNATIONAL COUNCIL
OF THE AERONAUTICAL SCIENCES
STOCKHOLM, SWEDEN, 4-9 SEPTEMBER, 2022

ICAS 2022 SWEDEN

COMPARISON OF ANALYTICAL SEMI-EMPIRICAL MODEL FOR JET-NOISE PREDICTION

Francesco Petrosino[1] & Mattia Barbarino[1]

[1]CIRA—Italian Aerospace Research Centre, Capua (CE), 81043, Italy

Abstract

The jet noise generation problem has been the subject of studies since the early 1950s, with the introduction of turbojets in commercial aircraft. Reduction of pollutants and noise motivated research efforts to predict and control the jet noise. The development of fast calculation tools for jet noise prediction could be a crucial factor in the design of high-speed aircraft. The main part of this work concerns the implementation of the James R. Stone's model, developed by Modern Technologies Corporation (MTC) for the National Aeronautics and Space Administration (NASA), in a modern numerical environment. Then a validation trough reproduction of test cases found in literature has been carried out, with a comparison between an early version of the model from 1983 and a newest version from 2009 published references.

Keywords: Aeroacoustics; Engine Noise; Jet Noise; Empirical method.

1. Introduction

The rapid growth of air and urban traffic has prompted Government commissions, the scientific community, and manufacturers to invest resources to reduce the environmental impact of their systems[1][2]. The design of next generation aircraft needs to include investigation on the generation of pollutants and noise, in order to reach the 2050 goals established by the European Commission. One of the results to achieve is a 65% (-15 EPNdB) for noise reduction[3].

More specifically, aircraft noise sources have several major components, one of which that is very important for take-off conditions is noise generated by the propulsive jet flow from the engine exhaust, identified with the term "jet noise"[4]. This phenomenon is related to noisy emissions that occur when a flow of combusted gas and air is released from the engine nozzle at a high speed compared to the external air field. The flow configuration is really complex, it is characterised by three-dimensional effects, non-linear velocity field, highly turbulent flows, intermittent phenomena, in some cases shock waves also. The entire jet noise prediction could be accomplished by a full unsteady CFD calculation[5], but the complexities associated with such a task for high Reynolds number jet flows mean that this is unlikely to be practical, especially in the design phase of an aircraft. To get faster predictions, a possible approach is to create a jet noise model based on experiments.

Stone proposed in the 1983[6] a development of further extensions and improvements to the low order jet noise model developed by Modern Technologies Corporation (MTC) for the National Aeronautics and Space Administration (NASA). This model was updated and corrected as published in 1999[7] and 2009[8]. The earlier and simpler version of the Stone's model (1983) was implemented in modern numerical framework. A first set of test case was simulated to check the correct implementation of the code. Then, the newest version of the model (2009) was inserted in the same numerical framework, using a additional set of test cases from the correspondent reference work of Stone.

This work is part of the European project SENECA[9], that will mainly focus on noise and emissions in the vicinity of airports and the global climate impact of supersonic aircraft.

Particularly, in Section 2. the model for jet-noise prediction is described. In addition, an outline of test performed is given. The main results are provided in Section 3. Finally, the most important conclusions extracted from this study are pointed out in Section 4.

2. Jet noise modelling

Jet-noise is the field of aeroacoustics problems that focuses on noise generated by high-speed jets flow and turbulent vortices, due to the aerodynamic shear layer.
More specifically, the term 'jet-noise' identifies all the phenomena of noisy emissions that occur when a flow of air is released from the engine nozzle at a high speed compared to the surrounding environment. However, the mechanisms behind the noise emission are not yet fully exploited. The flow configuration is complex, characterised by a highly three-dimensional effect, non-linear velocity field and intermittent phenomena [4].
The traditional statistical approach of Reynolds to approximate the turbulence in the aerodynamic flow decomposing every physical quantity of the turbulent field into a mean and a fluctuating component, is useful both to model the macroscopic characteristics of the turbulent flow and to make predictions on noise generation. However, this approach does not allow to describe the fluctuating quantities accurately, while many of the mechanisms that govern noise generation are related to the latter.
Classical approach to analyse the jet-noise is to separate the contributions: jet mixing noise is the one related to the shear flow between the flow exit the nozzle and the exterior free air, and shock associated noise that is the result of supersonic exit flow, as in Figure 1. Other acoustic sources within the jet pipe also contribute to noise generation, especially at low speeds, which includes combustion noise and sounds produced by the interactions of a turbulent flow with fans, compressors and turbine systems, but we don't take them into account in the present work.

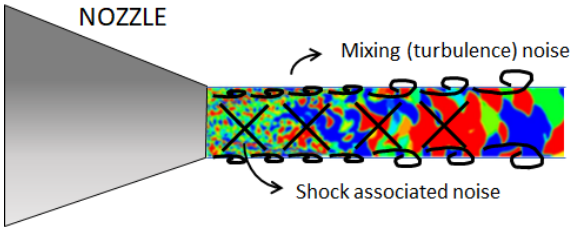

Figure 1 – Jet Noise sources.

2.1 Jet mixing noise

Jet mixing noise is created by the turbulent mixing of a flow ejected from the engine with the ambient fluid, which in most cases is air. The mixing initially takes place in an annular shear layer, which increases with the length of the nozzle. The mixing zone generally comprises the entire jet up to four or five diameters from the nozzle. The high-frequency components are mainly located near the nozzle, where the size of the turbulence vortices is small. The low-frequency zone, on the other hand, begins further downstream of the jet, where the size of the vortices is similar to the jet diameter.
From a physical point of view, the flow of a jet produces pressure fluctuations, related to the dynamics of both organised vortical structures and less regular random structures. Only a small portion of the energy associated with these fluctuations actually translates into pressure perturbations that propagate with the typical characteristics of sound. By examining the acoustic emission field of a turbulent jet, it can pointed out that the acoustic energy is distributed over a wide range of frequencies, which means that all turbulent structures, from large to small scale, are involved in the generation of sound. The focal point of research in this field is the intimate understanding of the mechanisms of noise production by each turbulent structure as it evolves in the fluid field. The full knowledge of the causes would allow engineering solutions to intervene directly on the causes of the noise by modifying the flow, with final goal to reduce the noise pollution of aircraft near airports, and also the preferred way to increase cabin comfort.
The aim of several works is to develop new methodological proposals for the analysis of turbulent jet data, which allow the correlation of the acoustic pressure fluctuations with the phenomena originating in the fluid field. A jet is a flow that is introduced into an environment under stationary conditions, creating an interaction that results in intense mixing and a flow layer, which becomes larger and larger as you move along the jet axis. The conical area between the outlet section and the point where the flow layer meets the axis of the jet is known as the potential core.

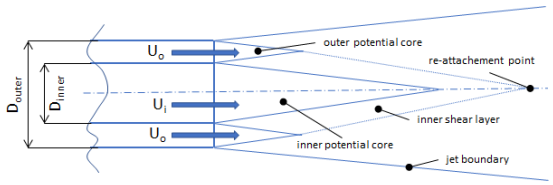

Figure 2 – Design of a coaxial jet.

However, the flow configuration that comes closest to the construction reality of the turbofan engines currently in use in most commercial aircraft is the coaxial jet. In this case, two flows, generally at different velocities, are introduced into the environment through as many coaxial outlet sections. This complicates the topology of the flow,which therefore has an inner potential core and an outer potential core, which then interact with each other, as in Figure 2. The potential core of the main jet has an extension that is strongly dependent on the velocity ratio between the main and secondary jets[10]), a quantity that also governs the velocity decay law along the jet axis.

2.2 Shock associated noise

In supersonic jets there are cells through which the flow expands and contracts continuously. Many of these "shock cells" can extend up to ten jet diameters from the nozzle and are responsible for two additional jet noise components, namely "screech tones" and "broadband shock associated noises". Screech tones from supersonic jets are generated by a feedback mechanism in which a convective disturbance in the shear layer generates the sound as it passes through the permanent shock wave system of the jet. The feedback loop consists of three main components: the downstream propagation of the wave instability, the shock cell structure in the jet plume, and the in the jet plume and the feedback of the acoustic waves immediately outside the jet. Screech is a side effect of the jet in flight and can be suppressed by an appropriate nozzle design.

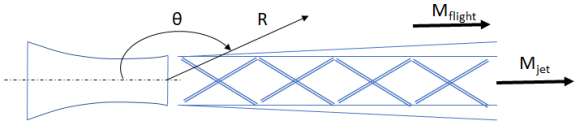

Figure 3 – Sketch of shock noise.

Broadband shock associated noises (BBSAN), as in Figure 3 are present in supersonic jets when the jet is operating in an off-design condition[11]. This is due to the fact that the static pressure at the nozzle outlet is not equal to the pressure outside of the nozzle. Nozzles operating at the nominal design pressure ratio can also create a periodic shock cell structure in the spray plume if the characteristic waves are not cancelled by the spray walls. BBSAN occurs in nozzles that are convergent or convergent-divergent when the flow is over- or under-expanded. BBSAN is observed in the far field as a broad spectral peak and dominates the jet mixing noise levels at large angles to the jet axis. The peak frequency is a function of the distance between shock cells in the jet, the convection velocity of the jet shear layer turbulence and also the position of the observer. The amplitude of the BBSAN depends on the ratio between the distance of the observer to the jet diameter, the polar and azimuthal observation angles, the nozzle geometry, the degree of off-design operation and to a lesser extent the stagnation temperature.

2.3 Stone's model

The National Aeronautics and Space Administration (NASA) has long been engaged in aircraft noise research and technology development, and has even conducted engine system testing and even flying tests on occasion. Since 1995, the Modern Technologies Corporation (MTC) has been creating practical and easy-to-use semi-empirical prediction models for jet noise to assist NASA and the aviation propulsion sector. The result of this project is currently part of General Electric's (GE) design and data reduction software, as well as the NASA Langley Research Center's (LaRC) Aircraft

Noise Prediction Program (ANOPP)[12] and NASA Glenn Research Center's (GRC) Footprint/Radius (FOOTPR)[13] code.

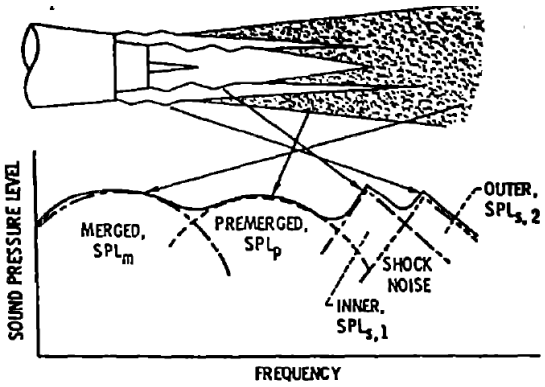

Figure 4 – Stone's decomposition of jet Noise sources in 2009 model update, adaptation of [7].

The model dedicated to jet-noise prediction was mainly developed by J. R. Stone[14]. Following the approach of figure 1 and figure 4, Stone breaks down the noise component due to turbulent mixing into further components. The lowest frequency component, generated well downstream of the nozzle exit, is most likely due to the mixing of the coherent large-scale turbulent structures of the jet with the ambient; so, it is called "large scale mixing noise," denoted by the subscript "L". The relatively high frequency mixing noise generated near the nozzle exit, is likely due to the small-scale turbulent mixing in the initial shear layer, it is called "small scale mixing noise," denoted by the subscript S. The most difficult to characterize mixing noise component, needed to completely correlate dual-stream mixing noise, occurs primarily at middle-to-high frequency. This component is called "transitional/intermediate scale mixing noise," denoted by the subscript T. Thus this last component is used for coanular nozzle. As regards the broadband associated shock noise there are two components. The inner stream shock noise (subscript I,sh), applied to the case of single stream, and the outer-stream shock noise (subscript O,sh) used only for dual-stream configurations.
The source noise models were semi-empirical, using real physical scaling laws that are calibrated with measured test data. The data used were jet mixing and shock noise of single-stream and dual-stream nozzles over a very wide range of geometries and test conditions, including suppression modifications on either or both streams. The evolution of this prediction/analysis/correlation approach has been in a sense backward, from the complex to the simple; but from this approach a very robust capability is emerging. In this work we will point out only the differences among the 1983 and 2009 Stone's model, leaving the extended description of the models in the corresponding papers available online.
In the 1983 version of the model, Stone proposed an equation able to compute the noise uncorrected for refraction SPL, taking into account the area ratio, velocity ratio, temperature ratio between inner and outer stream:

$$SPL - UOL_I = 5 \cdot log\left(\frac{T_1}{T_2}\right) + 10 \cdot log\left[\left(1 - \frac{V_2}{V_1}\right)^m + 1.2 \cdot \frac{[1 + ((A_2 V_2^2)/(A_1 V_1^2))]^4}{[1 + (A_2/A_1)]^3}\right] \tag{1}$$

where subscript 1 is relative to fully expanded primary (inner) jet, while subscript 2 to the fully expanded secondary (outer) jet. The exponent m depends on area ratio following the relations:

$$\begin{aligned} m &= 1.1\sqrt{A_2/A_1} \quad for \quad A_2/A_1 < 29.7 \\ m &= 6.0 \quad for \quad A_2/A_1 \geq 29.7 \end{aligned} \tag{2}$$

The relative sound pressure level UOL_I for the inner or single stream is correlated as a function of

the effective directivity angle θ' and the logarithmic Strouhal number $logS$:

$$UOL_i = 141 + 10 \cdot log\left[\left(\frac{\rho_a}{\rho_{ISA}}\right)^2\left(\frac{c_a}{c_{ISA}}\right)^4\right] + 10 \cdot log\left(\frac{A_1}{R^2}\right) + 10 \cdot log\left(\frac{\rho_1}{\rho_a}\right)^{\omega} + 10 \cdot log\left(\frac{V_e}{c_a}\right)^{7.5}$$
$$-15 \cdot log[(1 + M_c \cos\theta)^2 + 0.04M_c^2] - 10 \cdot log[1 - M_0 \cos(\theta - \alpha)] + 3 \cdot log\left(\frac{2A_1}{\pi D_1^2} + \frac{1}{2}\right) \quad (3)$$

where the subscript a refers to ambient condition, 0 refers to the aircraft, V_e ω and M_c are modified velocities to take into account the relative speed between the aircraft and the engine. The variable θ is the directivity angle from the observer position to the engine inlet axis, R is the distance between observer and engine outlet. Stone identified in this model only a single component for the mixing noise contribution, named "merged" noise.
In the same way, Stone provided the contribution to noise due to shock presence. The expression of $UOL_{S,j}$ uncorrected for the refraction, and with the hypotheses of no interaction in case of two streams, is:

$$UOL_{S,j} = 162 + 10 \cdot log\left[\left(\frac{\rho_a}{\rho_{ISA}}\right)^2\left(\frac{c_a}{c_{ISA}}\right)^4\right] + 10 \cdot log\left(\frac{A_j}{R^2}\right) + 10 \cdot log\left[\frac{(M_j^2 - 1)^2}{1 + (M_j^2 - 1)^2}\right]$$
$$-10 \cdot log[1 - M_0 \cos(\theta - \alpha)] + F(\theta - \theta_M) \quad (4)$$

where the subscript j refers to 1 for the inner stream and 2 for the outer stream that is supersonic, θ_M is the Mach angle equal to $180(deg) - \sin^{-1}(1/M_j)$, while the function F is given by

$$F = 0 \quad for \quad \theta \leq \theta_M$$
$$F = -0.75 \quad for \quad \theta > \theta_M \quad (5)$$

Stone constructed a table of $SPL - UOL_I$ function of logarithm of Strouhal number and directivity angle, using a large amount of experimental data on different nozzle configurations, for both mixing and supersonic noise. Once defined the directivity angle θ and the Strouhal number, knowing the parameters of the jet (geometric inputs, operating conditions, ambient conditions), it is possible to extract the $SPL - UOL_I$ value from the tables, solve the equations 3 and 4, and finally obtain the SPL of the considered jet configuration, eventually using the equation 1 to make a correction in case of dual stream jet. This process is summarized in figure 5.

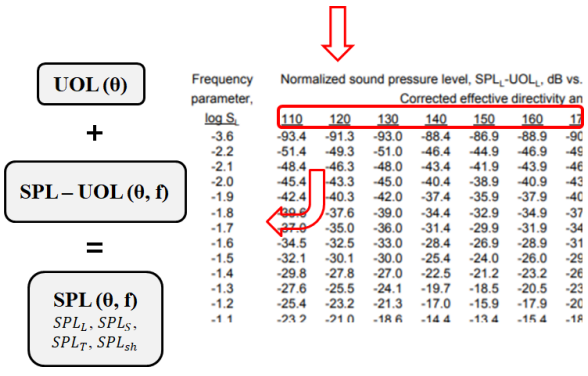

Figure 5 – Stone's model workflow.

Using the expression of the Strouhal number provided in the reference paper, that correlate the frequency and the characteristics of the jet with this adimensional number, it is possible to convert the results in terms of $1/3$ of octave bands.
In 2009 model update, Stone analysed several additional experiments, in particular engine with high by-pass ratio and external plugs. In particular, Stone separate the mixing noise contribution in three part: large scale (merged in previous version), small scale and transitional scale (pre-merged in previous version). The shock noise contribution is different depends on the zone of the shock, there

are inner stream (or single) shock noise and outer stream shock noise. The presence of the plug in the engine lead to other additional noise contribution: inner stream plug separation noise and plug (or downstream) shock noise, in case of supersonic flow after the plug. Comparing the 2009 model to the 1983 model we found 7 tables with spectral directivity relations instead of 2 tables. Also the equations of overall level uncorrected for refraction UOL for each component have some differences with the previously presented formulations. For the mixing noise contribution, the three formulation for the large, small and transitional scale are:

$$UOL_L = C_L + 10 \cdot log\left[\left(\frac{\rho_a}{\rho_{ISA}}\right)^2\left(\frac{c_a}{c_{ISA}}\right)^4\right] + 10 \cdot log\left(\frac{A_L}{R^2_{cor,L}}\right) + 10 \cdot log\left(\frac{\rho_L}{\rho_a}\right)^{\omega_L} \\ -20 \cdot log[(1 + M_{c,L}\cos\theta_{cor,L})^2 + 0.09M^2_{c,L}] \tag{6}$$

$$UOL_S = C_S + 10 \cdot log\left[\left(\frac{\rho_a}{\rho_{ISA}}\right)^2\left(\frac{c_a}{c_{ISA}}\right)^4\right] + 10 \cdot log\left(\frac{A_S}{R^2_{cor,S}}\right) + 10 \cdot log\left(\frac{\rho_S}{\rho_a}\right)^{\omega_S} \\ +75 \cdot log\left(\frac{V_{e,S}}{c_a}\right) - 20 \cdot log[(1 + M_{c,S}\cos\theta_{cor,S})^2 + 0.09M^2_{c,S}] \tag{7}$$

$$UOL_T = C_T + 10 \cdot log\left[\left(\frac{\rho_a}{\rho_{ISA}}\right)^2\left(\frac{c_a}{c_{ISA}}\right)^4\right] + 10 \cdot log\left(\frac{A_T}{R^2_{cor,T}}\right) + 10 \cdot log\left(\frac{\rho_T}{\rho_a}\right)^{\omega_T} \\ +75 \cdot log\left(\frac{V_{e,T}}{c_a}\right) - 20 \cdot log[(1 + M_{c,T}\cos\theta_{cor,T})^2 + 0.09M^2_{c,T}] \tag{8}$$

The variable R_{cor} is the distance observer-to-source that vary for each component, because the experimental jet noise measurements are typically made at a distance far enough from the nozzle to be in the far field of any individual noise source region, but not far enough away to treat the entire exhaust plume as a point source at the center of the nozzle exit plane, as assumed in the Stone previous model. The convective Mach number M_c, the effective velocity V_e and the density effect on noise correlated to the variable exponent ω also differ for each component, and depend on jet nozzle configuration and operating conditions. The coefficients C_L, C_S and C_T calculated with dedicated formulations, determined after analysing data coming from experiments. This is another huge difference against the 1983 model where the coefficient was fixed to the value 141 as in equation 3.
For inner or outer stream shock noise, when the flow is fully expanded supersonic, the noise component is calculated in the 2009 model using the following formulation:

$$UOL_{Sh,j} = C_{Sh,j} + 10 \cdot log\left[\left(\frac{\rho_a}{\rho_{ISA}}\right)^2\left(\frac{c_a}{c_{ISA}}\right)^4\right] + 10 \cdot log\left(\frac{A_j}{R^2_{cor,j}}\right) + 10 \cdot log\left[\beta_j^4/(1+\beta_j^4)\right] \\ -40 \cdot log\left[1 - M_0\cos\theta_{cor,j}\right] + F(\theta_{cor,j} - \theta_{M,j}) \tag{9}$$

where the subscript j refers to 1 for the inner stream and 2 for the outer stream that is supersonic, θ_M is the Mach angle equal to $180(deg) - \sin^{-1}(1/M_j)$, while the function F is given by

$$F = 0 \quad for \quad \theta_{cor,j} < \theta_{M,j} \\ F = -0.75(\theta_{cor,j} - \theta_{M,j}) \quad for \quad \theta_{cor,j} \geq \theta_{M,j} \tag{10}$$

and the shock strength parameter β_j is calculated as

$$\beta_j = \left[(M_j^2 - M_{d,j}^2)^2 + 0.01M_{d,j}/(1 - D_{1,j}/D_{2,j})\right]^{1/4} \tag{11}$$

M_d is the design Mach number of the nozzle, D_1 is the inner stream nozzle exit inner diameter and D_2 is the inner stream nozzle exit outer diameter. Comparing the equation 9 with the previous equation 4 the shock strength term is better evidenced, and the function F is defined including the values of directivity angles. Also in this case, the coefficient C_{sh} is defined using several formulation derived from experiments, against the fixed value of 162 in equation 4.

2.4 Test cases

In order to point out the differences between the Stone's model published in 1983 and the one published in 2009, several test cases were selected from the different articles of Stone, including different type of nozzles and flow conditions. The first test case is a coaxial coplanar nozzle from 1983 paper, with dual-stream flow, both subsonic, conditions reported in table 1. The second test case is a coaxial coplanar nozzle, from the same paper, with dual-stream flow with supersonic inner flow, conditions reported in table 2. The third test case is an inverted-velocity-profile coanular jet, that correspond to a dual-stream nozzle where the outer-stream velocity is higher than the inner stream, presented in an article published in 1999, containing a preliminary version of the 2009 model. The conditions of the third case are reported in table 3. The fourth test case is a coanular nozzle with external plug, from the more recent paper published in 2009, conditions reported in table 4.

Table 1 – Test case 1: Conventional profile jet mixing noise, figure 5 in reference[6]

	Case 1a	Case 1b	Case 1c	Case 1d
Ambient density [kg/m^3]	1.225			
Ambient speed of sound [m/s]	340.3			
Source to observer distance [m]	7.1	5.0	6.1	8.7
Inner stream density [kg/m^3]	0.369			
Outer stream density [kg/m^3]	1.377			
Inner stream velocity [m/s]	593			
Outer stream velocity [m/s]	216			
Inner stream Mach number	0.951			
Outer stream Mach number	0.678			
Inner stream diameter [m]	0.1010			
Outer stream inner diameter [m]	0.1090			
Outer stream outer diameter [m]	0.2096			
Inner stream total temperature [K]	1129			
Outer stream total temperature [K]	280			
Flight velocity [m/s]	0			
Angle of attack [deg]	0			
Theta Polar angle of emission [deg]	45	90	125	145

Table 2 – Test case 2: Conventional profile jet shock noise, figure 7a in reference[6]

	Case 2a	Case 2b	Case 2c
Ambient density [kg/m^3]	1.225		
Ambient speed of sound [m/s]	340.3		
Source to observer distance [m]	7.1		
Inner stream density [kg/m^3]	0.740	0.801	0.419
Outer stream density [kg/m^3]	1.377		
Inner stream velocity [m/s]	490	571	790
Outer stream velocity [m/s]	216		
Inner stream Mach number	1.13	1.37	1.38
Outer stream Mach number	0.678		
Inner stream diameter [m]	0.1010		
Outer stream inner diameter [m]	0.1090		
Outer stream outer diameter [m]	0.2096		
Inner stream total temperature [K]	592	594	1124
Outer stream total temperature [K]	280		
Flight velocity [m/s]	0		
Angle of attack [deg]	0		
Theta Polar angle of emission [deg]	45		

Table 3 – Test case 3: IVP jet noise, figure 7 in reference[7]

	Case 3a	Case 3b	Case 3c	Case 3d
Ambient density [kg/m^3]	1.225			
Ambient speed of sound [m/s]	337.9			
Source to observer distance [m]	12.2			
Inner stream density [kg/m^3]	0.716			
Outer stream density [kg/m^3]	0.675			
Inner stream velocity [m/s]	367			
Outer stream velocity [m/s]	548			
Inner stream Mach number	0.828			
Outer stream Mach number	1.200			
Inner stream diameter [m]	0.11788			
Outer stream inner diameter [m]	0.12195			
Outer stream outer diameter [m]	0.15488			
Inner stream total temperature [K]	553			
Outer stream total temperature [K]	664			
Flight velocity [m/s]	0			
Angle of attack [deg]	0			
Theta Polar angle of emission [deg]	60	90	120	140

Table 4 – Test case 4: External plug nozzle jet mixing noise, figure 24 in reference[8]

	Case 4a	Case 4b	Case 4c	Case 4d
Ambient density [kg/m^3]	1.239			
Ambient speed of sound [m/s]	336.3			
Source to observer distance [m]	12.2			
Inner stream density [kg/m^3]	0.483			
Outer stream density [kg/m^3]	1.240			
Inner stream velocity [m/s]	481.56			
Outer stream velocity [m/s]	326.42			
Inner stream Mach number	0.895			
Outer stream Mach number	0.971			
Inner stream inner diameter [m]	0.70965			
Inner stream outer diameter [m]	1.0477			
Outer stream inner diameter [m]	1.5077			
Outer stream outer diameter [m]	1.9566			
Inner stream total temperature [K]	833.71			
Outer stream total temperature [K]	333.71			
Flight velocity [m/s]	67.25			
Angle of attack [deg]	0			
Theta Polar angle of emission [deg]	55	90	125	145
Distance primary exit plane to plug tip [m]	1.12			
Plug tip radius [m]	0.05			

An example of the numerical results obtained with the Stone's model are presented in figure 6. The picture 6(a) represents the sound pressure levels varying with the noise frequencies in the case of supersonic nozzle, extracted from the early model of 1983. The total curve is the result of the Stone model, sum of the contribution due to turbulence (mixing noise, with label jet in the picture) and the contribution of the shock presence. The semi-empirical model is in good agreement with the experiments in the low frequencies region, but overestimate in the high frequencies part. Looking at the picture 6(b), that is the latest model of 2009, sound pressure level of coanular nozzle with external plug is presented comparing numerical and experimental results. In the figure, the contribution to the

mixing noise of each turbulence scale is evidenced, with the plug noise contribution present in the high frequency region. The Stone's model is in good agreement in the medium and high frequency zones, but it is underestimating the low frequency results.
Stone itself remarks in his publications the difficulties in analysing the experimental results, due to the complexity of the geometries, the several noise sources present (valves, elbows, obstructions, combustor) and the uncertainty of instrumentation.

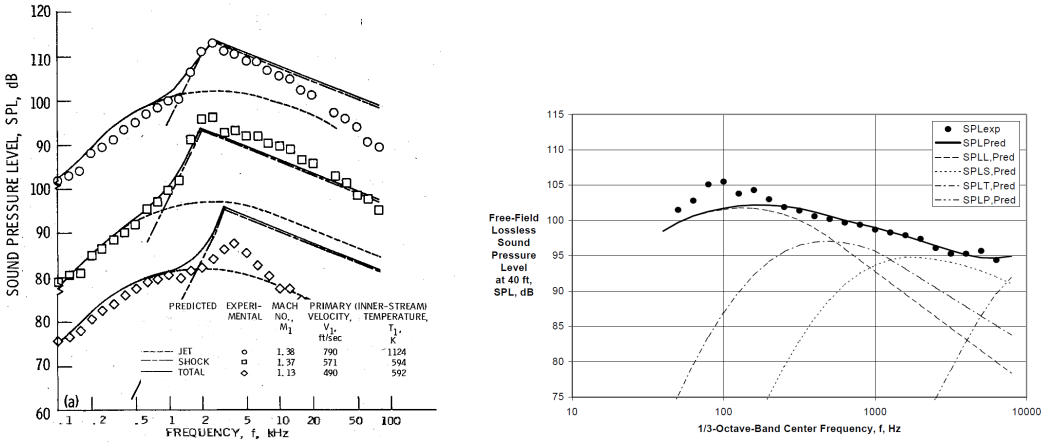

(a) Test case 2a-2b-2c, table 2.

(b) Test case 4a, table 4.

Figure 6 – Test cases selected from 1983 (6(a)) and 2009 (6(b) published works, adaptation of [6] and [8].

3. Results

The two Stone's models considered in this work, keep similar mathematical construction for all the noise components, with specific values for some of the coefficients defined to fit the experimental curves. The newest model is more complex compared to the previous version, it involves a huge experimental data set to account for different nozzle configurations, single and dual-stream, with and without shock waves, and for the presence of plug in the inner nozzle. Both the model were implemented in a modern numerical framework, following the scheme presented in figure 7. All the spectral directivity tables reported in the published works of Stone were inserted, as for the mathematical equation to calculate the noise coefficients. The user needs to add the geometric characteristics of the nozzle, the operating and ambient conditions. The code gives in output the jet noise predicted curves, each component of mixing, shock or plug, their sum, in terms of frequencies.

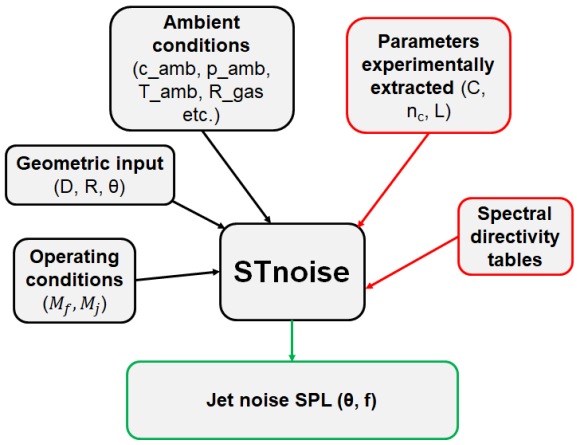

Figure 7 – Stone's model implementation in STNoise numerical tool.

The results of the test case 1 reported in table 1 are presented in figure 8. The red curve with label "CIRA_v09" correspond to Stone's model published in 2009, while the green curve with label

"CIRA_v08" refers to Stone's model published in 1983. Our numerical implementation of 1983 model is in perfect agreement with the curve presented by Stone. The newest model shows good agreement in the high frequency region, but poor adherence with the experiment in the low and medium frequency zones. The early model was constructed based on those experiments, while the newest is based on more contemporary engines, with high by-pass ratio and greater jet velocity, and consequently more noise in the high frequency range.

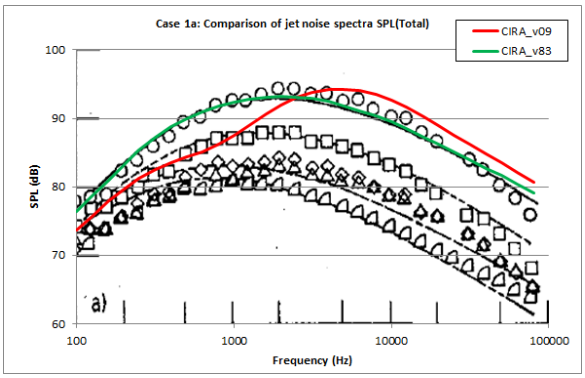

(a) Test case 1a.

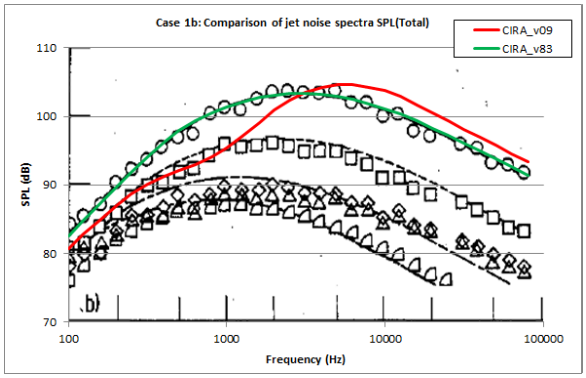

(b) Test case 1b.

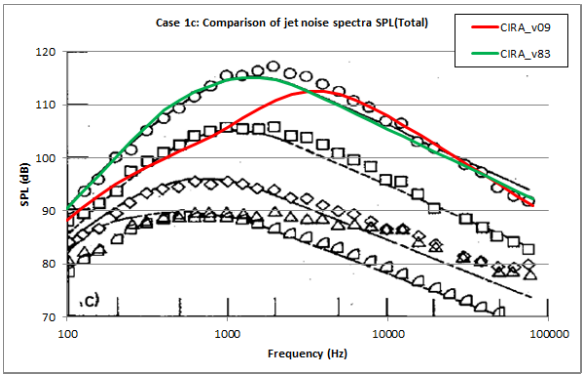

(c) Test case 1c.

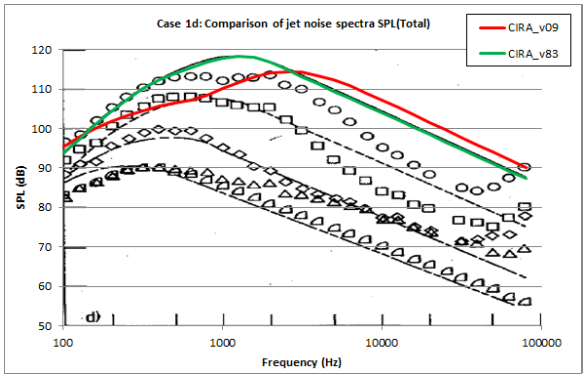

(d) Test case 1d.

Figure 8 – Test cases 1, reference table 1 and paper [6], different models.

The second set of cases presented in table 2 are shown in figure 9. Also in this case with a supersonic nozzle, the model from 1983 is in perfect agreement with the original implementation of Stone. In the high frequency part, this model tends to overestimate the noise respect to the experiments results. The model from 2009 shows a better agreement than 1983 model against the experiments, in the high frequency zone, where we expect better performance of the newest model.
The third test case results, related to table 3 and shown in the figure 10, and the fourth test case results, related to table 4 and shown in figure 11, are made with the model from 2009 only, because the model from 1983 is not able to simulate those nozzle configurations. Regarding the inverted-velocity-profile nozzle of test case 3, the model 2009 curve shows a similar shape compared to the experiments, even if there is a general overestimation of the values. As pointed out by Stone, in this particular test case was difficult to evaluate the operating condition and the geometric variables, and this leads to difficulties in select the right values in the numerical model.
The last test case in figure 11 was extracted from the published paper that is our reference for the 2009 model implementation. The numerical results are in very good agreement with the Stone curve, and also with the experiments. This particular case shows the effect of the external plug nozzle, in the high frequency zone, good predicted by the semi-empirical procedure presented.

4. Conclusions

The present work illustrates the implementation of a semi-empirical model developed by Stone, that is able to predict the jet noise generated by propulsive systems with different nozzle configuration,

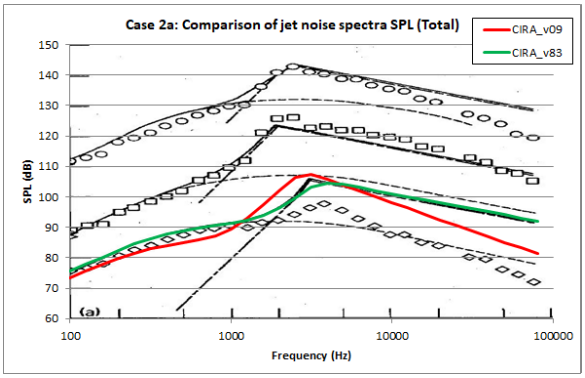

(a) Test case 2a.

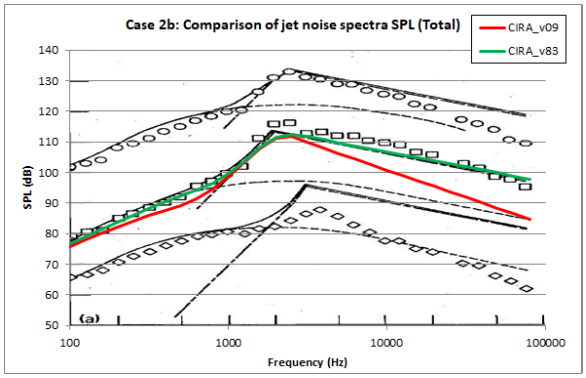

(b) Test case 2b.

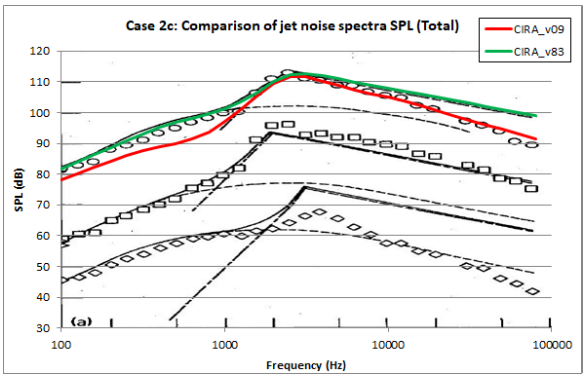

(c) Test case 2c.

Figure 9 – Test cases 2, reference table 2 and paper [6], different models.

single or dual stream, subsonic and supersonic ejected flow.
One of the first low-order jet-noise model was published in 1983, further extensions and improvements were published in 1999 and 2009. The model of 1983 and 2009 were implemented in modern numerical framework. The strength of this code is that it allows to estimate instantly the jet noise emissions, knowing the geometric parameters and the operating conditions only, over a very wide range of geometries and ambient conditions.
A first set of test case was simulated to check the correct implementation of the code, and point out the difference between the two models. Then, the newest version of the model (2009) was additionally tested using more complex geometries and conditions.
Despite the differences in the predicted noise field, the Stone's model is a very simple and fast procedure, that can be applied in the first phase of aircraft design to estimate the jet noise with reasonably accuracy, providing a guide results in the design stage of an aircraft.

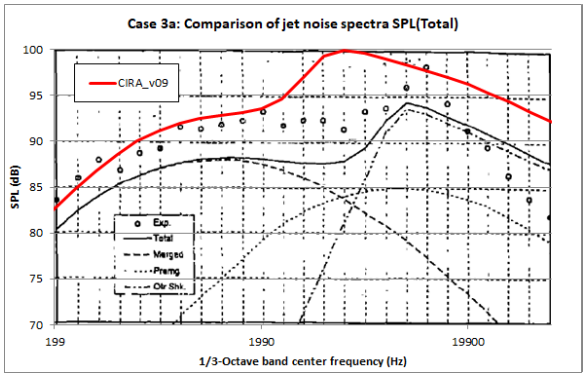

(a) Test case 3a.

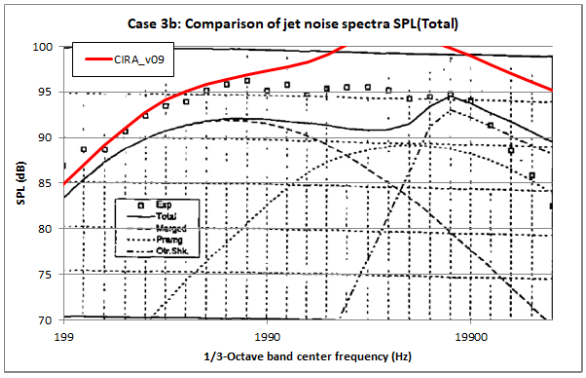

(b) Test case 3b.

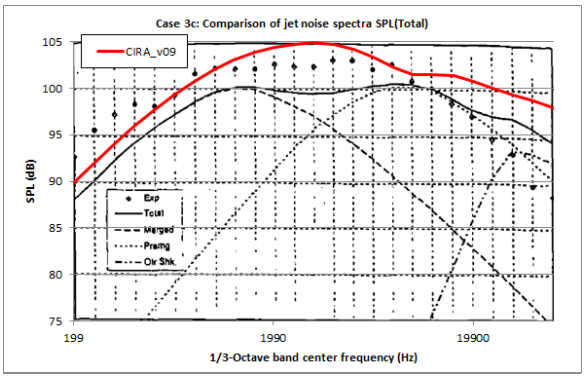

(c) Test case 3c.

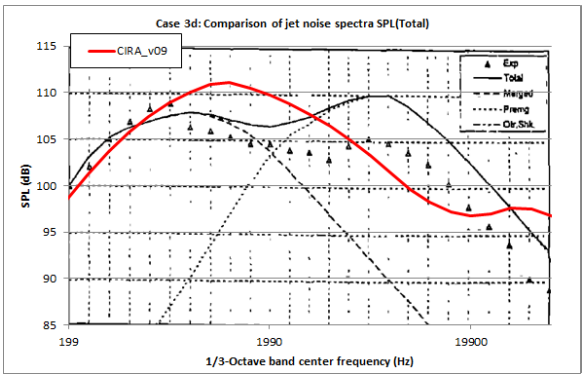

(d) Test case 3d.

Figure 10 – Test cases 3, reference table 3 and paper [7], Stone's model from 2009 paper [8].

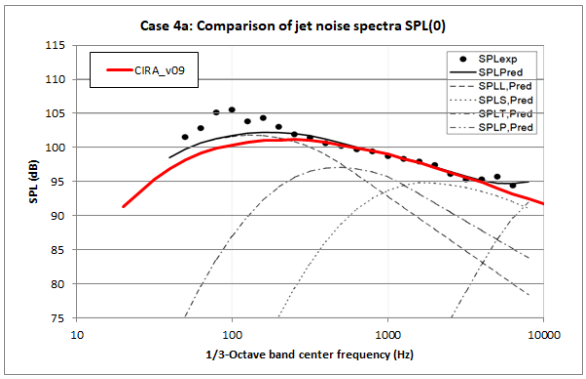

(a) Test case 4a.

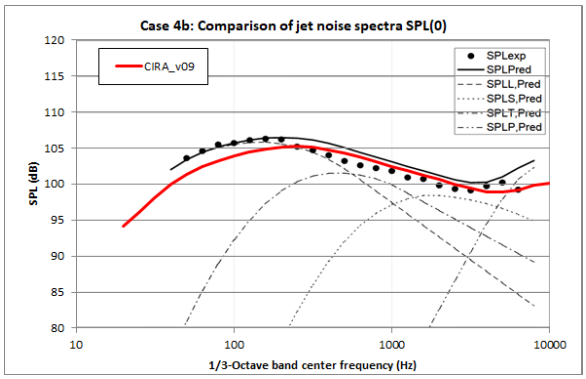

(b) Test case 4b.

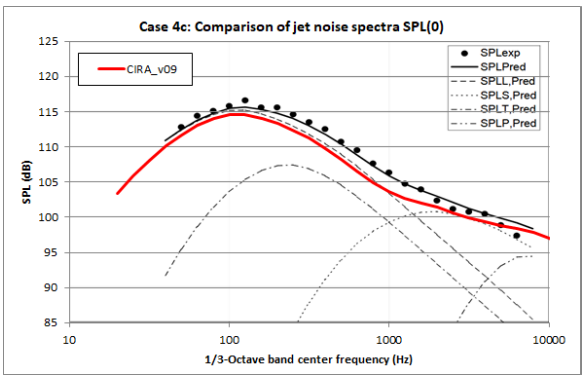

(c) Test case 4c.

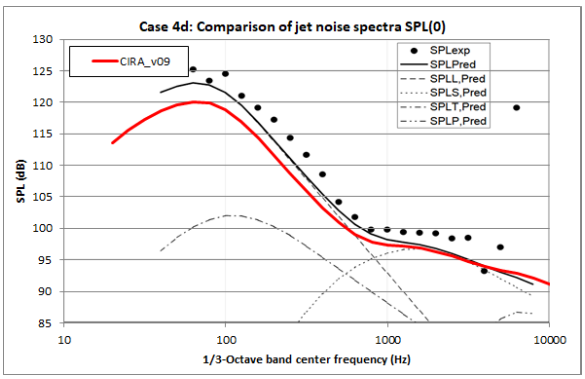

(d) Test case 4d.

Figure 11 – Test cases 4, reference table 4 and paper [8], Stone's model from 2009 paper [8].

5. Contact Author Email Address

Mail to: f.petrosino@cira.it

6. Funding

This research was funded by the European Union's Horizon 2020 research and innovation programme under grant agreement No. 101006742, project SENECA ((LTO) Noise and Emissions of Supersonic Aircraft).

7. Acknowledgments

Authors would like to thank all the partners of SENECA project, in particular Remco Habing from NLR for the coordination of the work, Robert Jaron from DLR and Maxime Huet from ONERA for the extrapolation of the test cases from the literature, Florian Kroemer from MTU for the management of activities, and all the people involved in the jet-noise modelling.

8. Copyright Statement

References

[1] World Health Organization. Environmental noise guidelines for the european region. 2018.

[2] B. Stoufflet C. Lorence F. Preli P. Stein E. Dalbies S. Klauke, N. Hussain. The sustainability of aviation, a statement of the chief technology officers of seven of the world's major aviation manufacturers. London, 2021.

[3] EU Commission. European green deal. 2019.

[4] Franck Kerhervé, Antoine Guitton, Peter Jordan, Joel Delville, Véronique Fortuné, Yves Gervais, and Charles Tinney. Identifying the dynamics underlying the large-scale and fine-scale jetnoise similarity spectra. 14th AIAA/CEAS Aeroacoustics Conference (29th AIAA Aeroacoustics Conference), 2008.

[5] Mattia Barbarino, Mario Ilsami, Raffaele Tuccillo, and Luigi Federico. Combined cfd-stochastic analysis of an active fluidic injection system for jet noise reduction. Applied Sciences, 7(6), 2017.

[6] James R. Stone, Donald E. Groesbeck, and Charles L. Zola. Conventional profile coaxial jet noise prediction. AIAA Journal, 21(3):336–342, 1983.

[7] James Stone, Charles Zola, and Bruce Clark. An improved model for conventional and inverted-velocity-profile coannular jet noise. 37th Aerospace Sciences Meeting and Exhibit, 1999.

[8] BJ Clark JR Stone, EA Krejsa and JJ Berton. Jet noise modeling for suppressed and unsuppressed aircraft in simulated flight. NASA Technical Memorandum, NASA-TM-2009-215524, 2009.

[9] SENECA. Lto noise and emissions of supersonic aircraft. European Union's Horizon 2020 research and innovation program, Grant No 101006742, 2021.

[10] H.A. Warda, S.Z. Kassab, K.A. Elshorbagy, and E.A. Elsaadawy. An experimental investigation of the near-field region of a free turbulent coaxial jet using lda. Flow Measurement and Instrumentation, 10(1):15–26, 1999.

[11] Christopher K. W. Tam. Broadband shock associated noise from supersonic jets measured by a ground observer. AIAA Journal, 30(10):2395–2401, 1992.

[12] W. E. Zorumski. Aircraft noise prediction program theoretical manual, part 1. NASA Technical Memorandum, NASA-TM-83199-PT-1, 1982.

[13] B. J. Clark. Computer program to predict aircraft noise levels. NASA Technical Publication, NASA-TP-1913, 1981.

[14] F. J. Montegani J. R. Stone. An improved prediction method for the noise generated in flight by circular jets. NASA Technical Memorandum, NASA-TM-81470, 1980.